JACS
JOURNAL OF THE AMERICAN CHEMICAL SOCIETY

Communication

Tunneling Controls the Reaction Pathway in the Deformylation of Aldehydes by a Nonheme Iron(III)-Hydroperoxo Complex: Hydrogen Atom Abstraction versus Nucleophilic Addition

Seong Hee Bae, Xiao-Xi Li, Mi Sook Seo, Yong-Min Lee, Shunichi Fukuzumi, and Wonwoo Nam

J. Am. Chem. Soc., **Just Accepted Manuscript** • Publication Date (Web): 29 Apr 2019

ACS Publications

is published by the American Chemical Society. 1155 Sixteenth Street N.W., Washington, DC 20036

Tunneling Controls the Reaction Pathway in the Deformylation of Aldehydes by a Nonheme Iron(III)-Hydroperoxo Complex: Hydrogen Atom Abstraction versus Nucleophilic Addition

Seong Hee Bae,[†] Xiao-Xi Li,[†] Mi Sook Seo,[†] Yong-Min Lee,[†] Shunichi Fukuzumi,*[,†,‡] and Wonwoo Nam*[,†,§]

[†]Department of Chemistry and Nano Science, Ewha Womans University, Seoul 03760, Korea

[‡]Faculty of Science and Engineering, Meijo University, SENTAN, Japan Science and Technology Agency (JST), Nagoya, Aichi 468-8502, Japan

[§]State Key Laboratory for Oxo Synthesis and Selective Oxidation, Suzhou Research Institute of LICP, Lanzhou Institute of Chemical Physics (LICP), Chinese Academy of Sciences, Lanzhou 730000, China

Supporting Information Placeholder

ABSTRACT: Mononuclear nonheme iron(III)-hydroperoxo intermediates play key roles in biological oxidation reactions. In the present study, we report a highly intriguing reactivity of a nonheme iron(III)-hydroperoxo complex, $[(TMC)Fe^{III}(OOH)]^{2+}$ (**1**), in the deformylation of aldehydes, such as 2-phenylpropionaldehyde (2-PPA) and its derivatives; that is, the reaction pathway of the aldehyde deformylation by **1** varies depending on reaction conditions, such as temperature and substrate. At temperature above 248 K, the aldehyde deformylation occurs predominantly via a nucleophilic addition (NA) pathway. However, as the reaction temperature is lowered, the reaction pathway changes to a hydrogen atom transfer (HAT) pathway. Interestingly, the reaction rate becomes independent of temperature below 233 K with a huge kinetic isotope effect (KIE) value of 93 at 203 K, suggesting that the HAT reaction results from tunneling. In contrast, reactions with a deuterated 2-PPA at the α-position and 2-methyl-2-phenylpropionaldehyde proceed exclusively via a NA pathway irrespective of the reaction temperature. We conclude that the bifurcation pathways between NA and HAT result from the tunneling effect in the HAT reaction by **1**. To the best of our knowledge, this study reports the first example showing that tunneling plays a significant role in the activation of substrate C-H bonds by a mononuclear nonheme iron(III)-hydroperoxo complex.

Oxygen-containing iron species, such as iron(III)-superoxo, iron(III)-peroxo, iron(III)-hydroperoxo, and iron(IV)-oxo, are key intermediates in the activation of dioxygen by mononuclear nonheme iron enzymes and their model compounds.[1,2] Among the iron-oxygen species, nonheme iron(III)-hydroperoxo intermediates have shown an interesting amphoteric reactivity in electrophilic and nucleophilic reactions,[3,4] compared to the nucleophilic reactivity of iron(III)-peroxo species[5] and the electrophilic reactivity of iron(IV)-oxo species.[2] Other metal-hydroperoxo complexes have also shown reactivities as electrophiles in hydrogen atom transfer (HAT) and oxygen atom transfer (OAT) reactions and as nucleophiles in aldehyde deformylation reactions.[6] However, chemical properties and reactivities of the nonheme metal-hydroperoxide intermediates are less clearly understood and remain to be elusive.

Scheme 1. Reaction Pathways, HAT vs NA, and Substrates Used in the Mechanistic Study of Aldehyde Deformylation by an Iron(III)-Hydroperoxo Intermediate

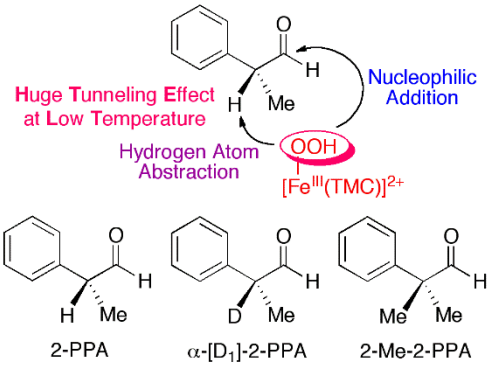

Very recently, Kumar, Sastri, de Visser, and their coworkers reported an interesting observation that a manganese(III)-peroxo complex reacts with 2-phenylpropionaldehyde (2-PPA) through a HAT pathway instead of the commonly proposed nucleophilic addition (NA) pathway in the deformylation of aldehydes by metal-peroxo species.[7] Evidence proposing the HAT mechanism in the deformylation of 2-PPA by the Mn(III)-peroxo complex was the kinetic isotope effect (KIE) value of ~5.4 when 2-PPA and a deuterated 2-PPA at the α-position (α-$[D_1]$-2-PPA) were used as substrates. In addition, 2-methyl-2-phenylpropionaldehyde (2-Me-2-PPA) did not react with the Mn(III)-peroxo complex. Thus, 2-PPA and its derivatives were shown to be excellent substrate probes that can be used in distinguishing the HAT vs NA pathways in oxidation reactions by metal-oxygen intermediates (Scheme 1).

In the present study, we have investigated the reactions of a mononuclear nonheme iron(III)-hydroperoxo complex, $[(TMC)Fe^{III}(OOH)]^{2+}$ (**1**, TMC = 1,4,8,11-tetramethyl-1,4,8,11-tetraazacyclotetradecane),[3a] with 2-PPA and its derivatives to address the following fundamental questions: (1) Are the HAT and NA pathways competing to each other in the

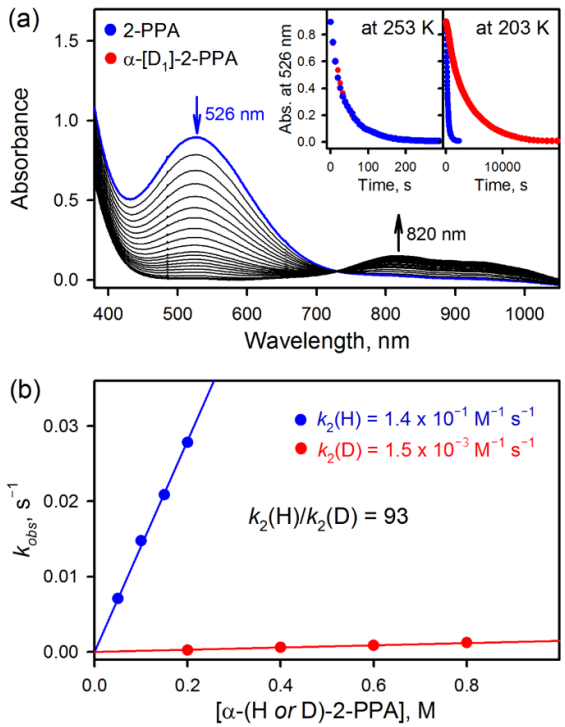

Figure 1. (a) UV-vis spectral changes observed in the reaction of **1** (0.50 mM) and 2-PPA (5.0 mM) in acetone/trifluoroethanol (v/v = 3:1) at 253 K. Insets show the time profiles for the decay of **1** in the reactions of **1** (0.50 mM) with 2-PPA (5.0 mM; blue circles) and α-[D1]-2-PPA (5.0 mM; red circles) at 253 K (left panel) and **1** (0.50 mM) with 2-PPA (20 mM; blue circle) and α-[D1]-2-PPA (200 mM; red circle) at 203 K (right panel). (b) Plots of pseudo-first-order rate constants (k_{obs}) vs concentrations of 2-PPA (blue circles) and α-[D1]-2-PPA (red circles) in the reactions of **1** with 2-PPA and α-[D1]-2-PPA at 203 K.

deformylation of aldehydes by **1** (i.e., HAT vs NA in Scheme 1)? (2) If yes, what are the reaction conditions that modulate the reaction pathways? (3) Then, why (and how) are the reaction pathways changed depending on the reaction conditions? We now report that the reaction pathway in the deformylation of aldehydes by **1** varies depending on the reaction conditions, such as temperature and substrate, and tunneling is an important factor that triggers the HAT reaction at low temperature. To the best of our knowledge, the present study reports the first example of tunneling effect that plays a significant role in the activation of substrate C-H bonds by a nonheme iron(III)-hydroperoxo complex.

The iron(III)-hydroperoxo complex, **1**, was prepared and characterized according to the published methods.[3a] Addition of 2-PPA to **1** in acetone/trifluoroethanol (v/v = 3:1) at 253 K under an Ar atmosphere resulted in the decay of **1** with the concurrent formation of $[(TMC)Fe^{IV}(O)]^{2+}$ (Figure 1a). The $[(TMC)Fe^{IV}(O)]^{2+}$ product was characterized using electron paramagnetic resonance (EPR) spectroscopy and cold-spray ionization mass spectrometer (CSI-MS) (Supporting Information (SI), Figure S1); the yield of $[(TMC)Fe^{IV}(O)]^{2+}$ was ~100% based on the absorbance at 820 nm (ε = 400 M^{-1} cm^{-1} for **1**).[8] Similarly, **1** reacted with α-[D1]-2-PPA under the identical conditions, showing that the reaction rate and spectral changes were the same as those of the reaction of **1** with 2-PPA (see Figure 1a, inset (left panel); Figure S2); the second-order rate constants, k_2(H) and k_2(D), for the reactions of **1** with 2-PPA and α-[D1]-2-PPA, respectively, were determined to be

Table 1. Rate Constants, k_2(H) and k_2(D), Determined in the Reactions of **1** with 2-PPA and α-[D1]-2-PPA at Various Temperatures[a]

entry	temp. (K)	k_2(H) and k_2(D), M^{-1} s^{-1}		k_2(H)/k_2(D)
		2-PPA	α-[D1]-2-PPA	
1	263	3.0	3.0	1.0
2	268	1.7	1.7	1.0
3	253	1.0	1.0	1.0
4	248	7.3×10^{-1}	7.3×10^{-1}	1.0
5	243	4.3×10^{-1}	4.0×10^{-1}	1.1
6	238	2.9×10^{-1}	2.3×10^{-1}	1.3
7	233	1.9×10^{-1}	1.1×10^{-1}	1.7
8	228	1.7×10^{-1}	6.1×10^{-2}	2.8
9	223.	1.6×10^{-1}	3.4×10^{-2}	4.7
10	218	1.6×10^{-1}	1.8×10^{-2}	8.9
11	213	1.5×10^{-1}	8.0×10^{-3}	19
12	208	1.4×10^{-1}	3.8×10^{-3}	37
13	203	1.4×10^{-1}	1.5×10^{-3}	93

[a]See experimental conditions in SI, Experimental Section.

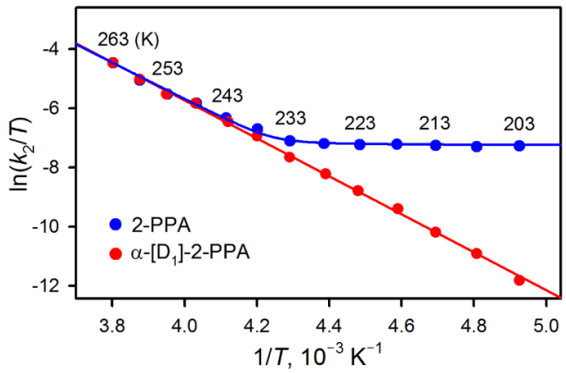

Figure 2. Eyring plots of $\ln(k_2/T)$ vs T^{-1} for the deformylation reactions of 2-PPA (blue circles) and α-[D1]-2-PPA (red circles) by **1**.

the same (i.e., 1.0 M^{-1} s^{-1} at 253 K) (Table 1, entry 3; Figure S3b). In addition, product analysis of the 2-PPA and α-[D1]-2-PPA reaction solutions revealed the formation of acetophenone as the product (85(4)% yield).

We also performed the reactions of **1** with 2-PPA and α-[D1]-2-PPA in the temperature range from 203 to 263 K; the k_2(H) and k_2(D) values were determined from the slopes of the linear plots of the pseudo-first-order rate constants vs concentrations of 2-PPA and α-[D1]-2-PPA (Table 1; Figure S3). First, the k_2(H) and k_2(D) values determined at temperatures above 248 K were the same, giving the k_2(H)/k_2(D) ratio of 1.0 (Table 1, entries 1 – 4). Interestingly, as the reaction temperature was lowered, the k_2(D) values became smaller than the k_2(H) values, giving the k_2(H)/k_2(D) ratio of >1, and a large k_2(H)/k_2(D) ratio of 93 was obtained at 203 K (Table 1, entry 13; Figure 1b).

Further, as the Eyring plots are shown in Figure 2, a linear correlation of $\ln(k_2(D)/T)$ vs T^{-1} was observed in the reaction of **1** and α-[D1]-2-PPA in the whole temperature range (Figure 2, red circles), affording an activation enthalpy ($\Delta H^{\ddagger}$) of 13 kcal mol^{-1} and an activation entropy ($\Delta S^{\ddagger}$) of −8.5 cal mol^{-1} K^{-1}. Interestingly, in the reaction of **1** and 2-PPA, a linear correla-

Scheme 2. Reactions of 1 with 2-PPA and α-[D$_1$]-2-PPA Carried Out in the Presence of $^{18}O_2$ and CCl_3Br

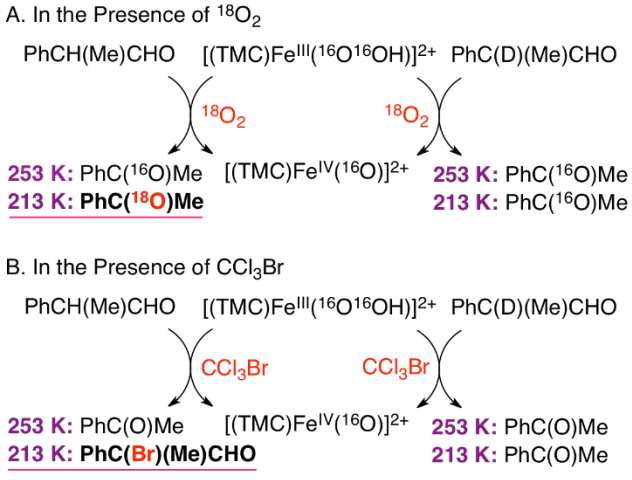

tion of $\ln(k_2(H)/T)$ vs T^{-1} was observed at temperatures above 248 K (Figure 2, blue circles) but curved from 248 K to 233 K. At temperatures below 233 K, the reaction rates, k_2(H), were temperature-independent (Figure 2, blue line). It is noted that the temperature insensitivity of the reaction rate with a large $k_2(H)/k_2(D)$ ratio is the indication of the involvement of tunneling (vide infra).[9-11]

Another substrate probe that we used in this mechanistic study was 2-methyl-2-phenylpropionaldehyde (2-Me-2-PPA) (see the structure in Scheme 1); Kumar, Sastri, de Visser, and their co-workers reported that their Mn(III)-peroxo complex did not react with 2-Me-2-PPA, since the Mn(III)-peroxo reacted with aldehyde solely via a HAT pathway.[7] In our study, however, a linear correlation of $\ln(k_2/T)$ vs T^{-1} was observed in the reaction of **1** and 2-Me-2-PPA (Figure S4 and Table S1); the low reactivity of 2-Me-2-PPA, compared to that of α-[D$_1$]-2-PPA, is probably due to a steric effect and/or an electronic effect of substrates in nucleophilic reactions (e.g., 2°-CHO for α-[D$_1$]-2-PPA vs 3°-CHO for 2-Me-2-PPA).

The results presented above are interpreted as follows: (1) In the reactions of **1** with α-[D$_1$]-2-PPA and 2-Me-2-PPA, the deformylation occurs solely via a NA pathway irrespective of reaction temperature. (2) In the reaction of **1** and 2-PPA, a NA pathway is dominant at the temperatures above 248 K, but a HAT pathway is being involved at the temperature below 243 K and becomes dominant at lower temperatures, affording large $k_2(H)/k_2(D)$ values (e.g., $k_2(H)/k_2(D)$ of 93 at 203 K) (Table 1; Figure 1b). Thus, based on the observations of a large $k_2(H)/k_2(D)$ ratio and the temperature insensitivity of the reaction rate at low temperatures, we propose that the reaction of **1** and 2-PPA occurs via a H-atom abstraction and tunneling plays a pivotal role in overriding the NA pathway.[12]

We then carried out the reactions of **1** with 2-PPA and α-[D$_1$]-2-PPA in the presence of $^{18}O_2$ at 253 K and found that no ^{18}O was incorporated into the acetophenone product (Figure S5b) (Scheme 2A); the [(TMC)Fe^{IV}(O)]$^{2+}$ product did not contain ^{18}O either (Figure S6a). Interestingly, when the reaction of **1** and 2-PPA was carried out in the presence of $^{18}O_2$ at 213 K, a significant amount of ^{18}O was found in the acetophenone product with the formation of [(TMC)Fe^{IV}(^{16}O)]$^{2+}$ (Scheme 2A; Figures S5d and S6b). However, no ^{18}O-incorporation into the acetophenone product was observed in the reaction of **1** and α-[D$_1$]-2-PPA at 213 and 253 K. Similarly, when the reactions of **1** with 2-PPA and α-[D$_1$]-2-PPA were carried out in the presence of CCl_3Br at 213 and 253 K, we observed the formation of a brominated 2-PPA product only in the reaction of **1** and 2-PPA at 213 K (Scheme 2B; Figures S7 and S8). Other reactions, such as the reaction of **1** and 2-PPA at 253 K and the reactions of **1** and α-[D$_1$]-2-PPA at 213 and 253 K, did not yield the brominated 2-PPA product but acetophenone as the product (Scheme 2B; Figures S7a and S9). Based on the results of the $^{18}O_2$ and CCl_3Br experiments, we propose that a carbon radical species was generated from a H-atom abstraction of 2-PPA by **1** at 213 K (see Scheme 3A).[13] In other reactions, such as the reaction of **1** and 2-PPA at 253 K and the reactions of **1** and α-[D$_1$]-2-PPA at 213 and 253 K, such a carbon radical species was not generated (see Scheme 3B). We therefore conclude that the reaction of **1** and 2-PPA at 213 K occurs via a HAT pathway (Scheme 3A), whereas the reaction of **1** and 2-PPA at 253 K and the reactions of **1** and α-[D$_1$]-2-PPA at 253 and 213 K occur via a NA pathway (Scheme 3B).

Scheme 3. Proposed Mechanisms for the Reactions of 1 with 2-PPA and α-[D$_1$]-2-PPA

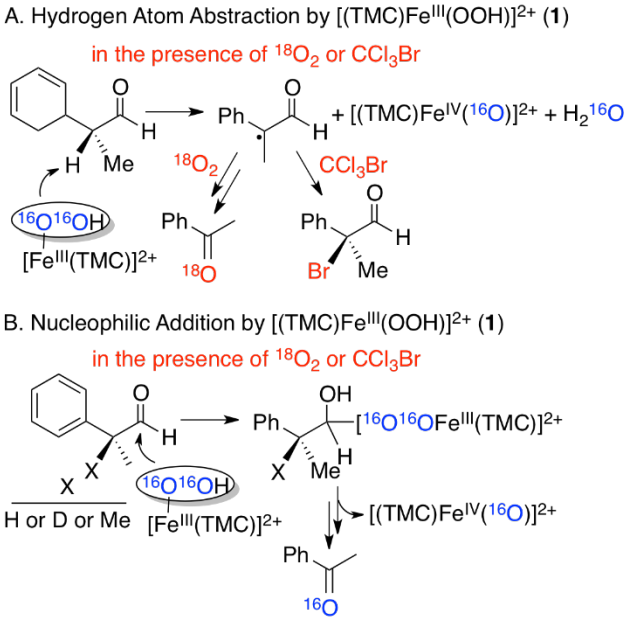

In conclusion, we have demonstrated that the reaction pathway in the deformylation of 2-PPA by a nonheme ion(III)-hydroperoxo complex (**1**) changes depending on reaction conditions, such as reaction temperature and substrate; (1) a HAT pathway in the reaction of **1** and 2-PPA at temperatures below 233 K and (2) a NA pathway in the reaction of **1** and 2-PPA at temperature above 248 K and in the reactions of **1** and 2-PPA derivatives (e.g., α-[D$_1$]-2-PPA and 2-Me-2-PPA) irrespective of reaction temperature. More importantly, we have shown that tunneling plays a significant role in the HAT reaction. Thus, this study has provided valuable insights into controlling the reaction pathway by tunneling effect as the third reactivity paradigm in addition to the thermodynamic and kinetic control.[14] In future study, we will attempt to elucidate the fundamental aspects of the tunneling effect on the C-H bond activation of hydrocarbons by nonheme iron-hydroperoxo intermediates as well as the detailed mechanisms of the HAT and NA pathways in the deformylation reaction by the nonheme iron(III)-hydroperoxo complex, **1**.

ASSOCIATED CONTENT

Supporting Information.
Experimental details, Table S1, and Figures S1 – S9. This material is available free of charge via the Internet at http://pubs.acs.org.

AUTHOR INFORMATION

Corresponding Author

wwnam@ewha.ac.kr
fukuzumi@chem.eng.osaka-u.ac.jp

Notes

The authors declare no competing financial interest.

ACKNOWLEDGMENT

This work was supported by the NRF of Korea through CRI (NRF-2012R1A3A2048842 to W.N) and Basic Science Research Program (2017R1D1A1B03029982 to Y.M.L. and 2017R1D1A1B03032615 to S.F.) and the Grants-in-Aid (no. 16H02268 to S.F.) from MEXT.

REFERENCES

(1) (a) Nam, W. Dioxygen Activation by Metalloenzymes and Models. *Acc. Chem. Res*. **2007**, *40*, 465. (b) Que, L., Jr. 60 Years of Dioxygen Activation. *J. Biol. Inorg. Chem.* **2017**, *22*, 171. (c) Solomon, E. I.; Goudarzi, S.; Sutherlin, K. D. O_2 Activation by Non-Heme Iron Enzymes. *Biochemisty* **2016**, *55*, 6363. (d) Jasniewski, A. J.; Que, L., Jr. Dioxygen Activation by Nonheme Diiron Enzymes: Diverse Dioxygen Adducts, High-Valent Intermediates, and Related Model Complexes. *Chem. Rev.* **2018**, *118*, 2554.

(2) (a) Guo, M.; Corona, T.; Ray, K.; Nam, W. Heme and Nonheme High-Valent Iron and Manganese Oxo Cores in Biological and Abiological Oxidation Reactions. *ACS Cent. Sci.* **2019**, *5*, 13. (b) Hong, S.; Lee, Y.-M.; Ray, K.; Nam, W. Dioxygen Activation Chemistry by Synthetic Mononuclear Nonheme Iron, Copper and Chromium Complexes. *Coord. Chem. Rev*. **2017**, *334*, 25. (c) Sahu, S.; Goldberg, D. P. Activation of Dioxygen by Iron and Manganese Complexes: A Heme and Nonheme Perspective. *J. Am. Chem. Soc*. **2016**, *138*, 11410. (d) Mondal, B.; Roy, L.; Neese, F.; Ye, S. High-Valent Iron–Oxo and –Nitrido Complexes: Bonding and Reactivity. *Isr. J. Chem.* **2016**, *56*, 763. (e) Engelmann, X.; Monte-Pérez, I.; Ray, K. Oxidation Reaction with Bioinspired Mononuclear Non-Heme Metal–Oxo Complexes. *Angew. Chem., Int. Ed*. **2016**, *55*, 7632. (f) Nam, W. Synthetic Mononuclear Nonheme Iron−Oxygen Intermediates. *Acc. Chem. Res*. **2015**, *48*, 2415. (g) Cook, S. A.; Borovik, A. S. Molecular Designs for Controlling the Local Environments around Metal Ions. *Acc. Chem. Res*. **2015**, *48*, 2407.

(3) (a) Cho, J.; Jeon, S.; Wilson, S. A.; Liu, L. V.; Kang, E. A.; Braymer, J. J.; Lim, M. H.; Hedman, B.; Hodgson, K. O.; Valentine, J. S.; Solomon, E. I.; Nam, W. Structure and Reactivity of a Mononuclear Non-Haem Iron(III)–Peroxo Complex. *Nature* **2011**, *478*, 502. (b) Liu, L. V.; Hong, S.; Cho, J.; Nam, W.; Solomon E. I. Comparison of High-Spin and Low-Spin Nonheme Fe^{III}–OOH Complexes in O–O Bond Homolysis and H-Atom Abstraction Reactivities. *J. Am. Chem. Soc*. **2013**, *135*, 3286. (c) Kim, Y. M.; Cho, K.-B.; Cho, J.; Wang, B.; Li, C.; Shaik, S.; Nam, W. A Mononuclear Non-Heme High-Spin Iron(III)–Hydroperoxo Complex as an Active Oxidant in Sulfoxidation Reactions. *J. Am. Chem. Soc*. **2013**, *135*, 8838. (d) Faponle, A. S.; Quesne, M. G.; Sastri, C. V.; Banse, F.; de Visser, S. P. Differences and Comparisons of the Properties and Reactivities of Iron(III)–Hydroperoxo Complexes with Saturated Coordination Sphere. *Chem.–Eur. J*. **2015**, *21*, 1221. (e) Wang, C.; Chen, H. Convergent Theoretical Prediction of Reactive Oxidant Structures in Diiron Arylamine Oxygenases AurF and CmII: Peroxo or Hydroperoxo? *J. Am. Chem. Soc*. **2017**, *139*, 13038.

(4) Sankaralingam, A.; Lee, Y.-M.; Nam, W.; Fukuzumi, S. Amphoteric Reactivity of Metal–Oxygen Complexes in Oxidation Reactions. *Coord. Chem. Rev*. **2018**, *365*, 41.

(5) Cho, J.; Sarangi, R.; Nam, W. Mononuclear Metal–O_2 Complexes Bearing Macrocyclic *N*-Tetramethylated Cyclam Ligands. *Acc. Chem. Res*. **2012**, *45*, 1321.

(6) (a) Sankaralingam, M.; Lee, Y.-M.; Jeon, S. H.; Seo, M. S.; Cho, K.-B.; Nam, W. A Mononuclear Manganese(III)–Hydroperoxo Complex: Synthesis by Activating Dioxygen and Reactivity in Electrophilic and Nuclerophilic Reactions. *Chem. Commun.* **2018**, *54*, 1209. (b) Shin, B.; Sutherlin, K. D.; Ohta, T.; Ogura, T.; Solomon, E. I.; Cho, J. Reactivity of a Cobalt(III)−Hydroperoxo Complex in Electrophilic Reactions. *Inorg. Chem*. **2016**, *55*, 12391. (c) Wang, C.-C.; Chang, H.-C.; Lai, Y.-C.; Fang, H.; Li, C.-C.; Hsu, H.-K.; Li, Z.-Y.; Lin, T.-S.; Kuo, T.-S.; Neese, F.; Ye, S.; Chiang, Y.-W.; Tsai, M.-L.; Liaw, W.-F.; Lee, W.-Z. A Structurally Characterized Nonheme Cobalt–Hydroperoxo Complex Derived from Its Superoxo Intermediate via Hydrogen Atom Abstraction. *J. Am. Chem. Soc*. **2016**, *138*, 14186. (d) Tcho, W.-Y.; Wang, B.; Lee, Y.-M.; Cho, K.-B.; Shearer, J.; Nam, W. A Mononuclear Nonheme Cobalt(III)–Hydroperoxide Complex with an Amphoteric Reactivity in Electrophilic and Nucleophilic Oxidative Reactions. *Dalton Trans*. **2016**, *45*, 14511. (e) Kim, S.; Ginsbach, J. W.; Lee, J. Y.; Peterson, R. L.; Liu, J. J.; Siegler, M. A.; Sarjeant, A. A.; Solomon, E. I.; Karlin, K. D. Amine Oxidative N-Dealkylation via Cupric Hydroperoxide Cu-OOH Homolytic Cleavage Followed by Site-Specific Fenton Chemistry. *J. Am. Chem. Soc*. **2015**, *137*, 2867. (f) So, H.; Park, Y. J.; Cho, K.-B.; Lee, Y.-M.; Seo, M. S.; Cho, J.; Sarangi, R.; Nam, W. Spectroscopic Characterization and Reactivity Studies of a Mononuclear Nonheme Mn(III)–Hydroperoxo Complex. *J. Am. Chem. Soc*. **2014**, *136*, 12229.

(7) (a) Barman, P.; Upadhyay, P.; Faponle, A. S.; Kumar, J.; Nag, S. S.; Kumar, D.; Sastri, C. V.; de Visser, S. P. Deformylation Reaction by a Nonheme Manganese(III)–Peroxo Complex via Initial Hydrogen-Atom Abstraction. *Angew. Chem., Int. Ed*. **2016**, *55*, 11091. (b) Reinhard, F. G. C.; Barman, P.; Mukherjee, G.; Kumar, J.; Kumar, D.; Kumar, D.; Sastri, C. V.; de Visser, S. P. Keto−Enol Tautomerization Triggers an Electrophilic Aldehyde Deformylation Reaction by a Nonheme Manganese(III)-Peroxo Complex. *J. Am. Chem. Soc.* **2017**, *139*, 18328.

(8) Rohde, J.-U.; In, J.-H.; Lim, M. H.; Brennessel, W. W.; Bukowski, M. R.; Stubna, A.; Münck, E.; Nam, W.; Que, L., Jr. Crystallographic and Spectroscopic Characterization of a Nonheme Fe(IV)=O Complex. *Science* **2003**, *299*, 1037.

(9) (a) Klinman, J. P.; Offenbacher, A. R. Understanding Biological Hydrogen Transfer Through the Lens of Temperature Dependent Kinetic Isotope Effects. *Acc. Chem. Res*. **2018**, *51*, 1966. (b) Meisner, J.; Kästner, J. Atom Tunneling in Chemistry. *Angew. Chem., Int. Ed*. **2016**, *55*, 5400. (c) Kohen, A. Role of Dynamics in Enzyme Catalysis: Substantial versus Semantic Controversies. *Acc. Chem. Res*. **2015**, *48*, 466. (d) Layfield, J. P.; Hammes-Schiffer, S. Hydrogen Tunneling in Enzymes and Biomimetic Models. *Chem. Rev.* **2014**, *114*, 3466. (e) Klinman, J. P. A New Model for the Origin of Kinetic Hydrogen Isotope Effects. *J. Phys. Org. Chem.* **2010**, *23*, 606. (f) Nagel, Z. D.; Klinman, J, P. Tunneling and Dynamics in Enzymatic Hydride Transfer. *Chem. Rev.* **2006**, *106*, 3095.

(10) (a) Mayer, J. M. Understanding Hydrogen Atom Transfer: Form Bond Strengths to Marcus Theory. *Acc. Chem. Res*. **2011**, *44*, 36. (b) Bowring, M. A.; Bradshaw, L. R.; Parada, G. A.; Pollock, T. P.; Fernández-Terán, R. J.; Kolmar, S. S.; Mercado, B. Q.; Schlenker, C. W.; Gamelin, D. R.; Mayer, J. M. Activationless Multiple-Site Concerted Proton−Electron Tunneling. *J. Am. Chem. Soc.* **2018**, *140*, 7449.

(11) (a) Mandal, D.; Mallick, D.; Shaik, S. Kinetic Isotope Effect Determination Probes the Spin of the Transition State, Its Stereochemistry, and Its Ligand Sphere in Hydrogen Abstraction Reactions of Oxoiron(IV) Complexes. *Acc. Chem. Res*. **2018**, *51*, 107. (b) Klein, J. E. M. N.; Mandal, D.; Ching, W.-M.; Mallick, D.; Que, L., Jr.; Shaik, S. Privileged Role of Thiolate as the Axial Ligand in Hydrogen Atom Transfer Reactions by Oxoiron(IV) Complexes in Shaping the Potential Energy Surface and Inducing Significant H-Atom Tunneling. *J. Am. Chem. Soc.* **2017**, *139*, 18705. (c) Mallick, D.; Shaik, S. Kinetic Isotope Effect Probes the Reactive Spin State, As Well As the Geometric Feature and Constitution of the Transition State during H-Abstraction by Heme Compound II Complexes. *J. Am. Chem. Soc.* **2017**, *139*, 11451. (d) Mandal, D.; Shaik, S. Interplay of Tunneling, Two-State Reactivity, and Bell–Evans–Polanyi Effects in C–H Activation by Nonheme Fe(IV)O Oxidants. *J. Am. Chem. Soc.* **2016**, *138*, 2094. (e) Mandal, D.; Ramanan, R.; Usharani, D.; Janardanan, D.; Wang, B.; Shaik, S. How Does Tunneling Contribute to Counterin-

tuitive H-Abstraction Reactivity of Nonheme Fe(IV)O Oxidants with Alkanes? *J. Am. Chem. Soc.* **2015**, *137*, 722.

(12) The change of reaction pathway depending on reaction temperature due to tunneling[9-11] has been reported recently in the oxidation of cyclohexene by an iron(IV)-oxo porphyrin π-cation radical species: Gupta, R.; Li, X.-X.; Cho, K.-B.; Guo, M.; Lee, Y.-M.; Wang, Y.; Fukuzumi, S.; Nam, W. Tunneling Effect That Changes the Reaction Pathway from Epoxidation to Hydroxylation in the Oxidation of Cyclohexene by a Compound I Model of Cytochrome P450. *J. Phys. Chem. Lett.* **2017**, *8*, 1557. It should be noted, however, that temperature independent rate constant due to complete tunneling that changes the selectivity and reactivity ordering as shown in Figure 2 is the first time to be demonstrated in this paper.

(13) Huang, X.; Groves, J. T. Beyond Ferryl-Mediated Hydroxylation: 40 Years of the Rebound Mechanism and C–H Activation. *J. Biol. Inorg. Chem.* **2017**, *22*, 185.

(14) Schreiner, P. R. Tunneling Control of Chemical Reactions: The Third Reactivity Paradigm. *J. Am. Chem. Soc.* **2017**, *139*, 15276.

TOC

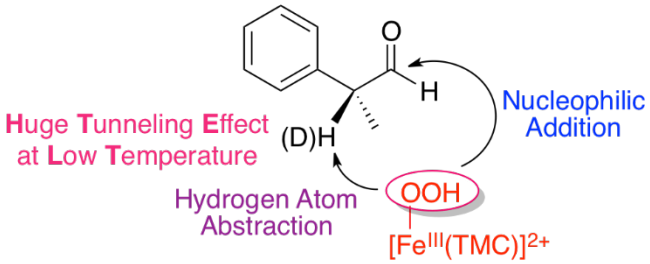
O
H
Nucleophilic
Addition
Huge Tunneling Effect
at Low Temperature
(D)H
Hydrogen Atom
Abstraction
OOH
[Fe^III(TMC)]^2+